New Journal of Physics
The open access journal at the forefront of physics

Deutsche Physikalische Gesellschaft DPG IOP Institute of Physics

PAPER • OPEN ACCESS

Controlling photonic spin Hall effect in graphene-dielectric structure by optical pumping

To cite this article: Peng Dong *et al* 2020 *New J. Phys.* **22** 113007

New Journal of Physics
The open access journal at the forefront of physics

Deutsche Physikalische Gesellschaft DPG
IOP Institute of Physics

Published in partnership with: Deutsche Physikalische Gesellschaft and the Institute of Physics

CrossMark

OPEN ACCESS

RECEIVED
25 August 2020

REVISED
23 October 2020

ACCEPTED FOR PUBLICATION
27 October 2020

PUBLISHED
6 November 2020

PAPER

Controlling photonic spin Hall effect in graphene-dielectric structure by optical pumping

Peng Dong[1,2,3], Jie Cheng[2], Haixia Da[1,3,*] and Xiaohong Yan[1,3,4,*]

[1] College of Electronic and Optical Engineering & College of Microelectronics, Nanjing University of Posts and Telecommunications, Nanjing 210023, Jiangsu, People's Republic of China
[2] School of Science, New Energy Technology Engineering Laboratory of Jiangsu Province, Nanjing University of Posts and Telecommunications, Nanjing 210023, Jiangsu, People's Republic of China
[3] Key Laboratory of Radio Frequency and Micro-Nano Electronics of Jiangsu Province, Nanjing 210023, Jiangsu, People's Republic of China
[4] School of Materials Science & Engineering, Jiangsu University, Zhenjiang 212013, Jiangsu, People's Republic of China
[*] Author to whom any correspondence should be addressed.

E-mail: eledah@njupt.edu.cn and yanxh@njupt.edu.cn

Keywords: photonic spin Hall effect, optical pumping, graphene, terahertz

Abstract

The photonic spin Hall effect (SHE) provides an effective way to manipulate the spin-polarized photons. However, the spin-dependent splitting is very tiny due to the weak spin–orbit coupling, and previous investigations for enhancing this phenomenon have some serious limitations (e.g. inconvenient to tune, inadequate attention in terahertz region). Therefore, controlling and enhancing the photonic SHE in a flexible way is highly desirable, especially for terahertz region. In this contribution, we propose a method to manipulate the photonic SHE by taking advantage of tunable optical properties of graphene via weak optical pumping. We find that photonic SHE of graphene-dielectric structure in terahertz region is quite sensitive to the pumping power. The spin shift for H polarized incident beam can reach its upper limitation under the optimal pumping power, which is related to the zero value of the real part of graphene conductivity. These findings may provide a new degree of freedom for the design of tunable spin-based photonic devices in the future.

1. Introduction

When a linear polarization beam propagates through inhomogeneous media, circularly polarized light (left- and right-handed circular polarizations) of opposite spin directions is separated in the lateral direction perpendicular to the incident surface [1–4]. This interesting phenomenon originating from spin–orbit interactions [3, 5] is called the photonic spin Hall effect (SHE). It can be regarded as a direct optical analogy of the SHE in an electronic system where the refractive index gradient plays the role of electric potential and the spin electrons are replaced by spin photons [1, 4]. Due to the profound physical connotations and potential applications in nano-photonics, the photonic SHE has attracted widespread attention since its discovery [6–9]. However, the photonic SHE is generally a very tiny phenomenon due to the weak spin–orbit coupling and the corresponding spin-dependent splitting is in the nanometer scale [10]. Therefore, several methods have been put forward to enhance the photonic SHE, which are based on Brewster angle [11, 12], surface plasmon resonance [13, 14], a parity-time symmetric system via exceptional point [15, 16] and so on [17, 18]. It should be noted that these methods have the intrinsic limitations, for instance, they are required to change the incident light beam or the parameters of device structures. Moreover, previous reports have focused on the photonic SHE in the visible and infrared ranges. Hence, controlling and enhancing the photonic SHE in a flexible way remains an open challenge, especially in the terahertz range, which is highly beneficial to facilitate its application in modern photonics.

Recently, a variety of novel materials (such as graphene [19], topological insulator [20], weyl semimetal [21], black phosphorus [22, 23]) hold great promise in the rapid development of photonic SHE and the

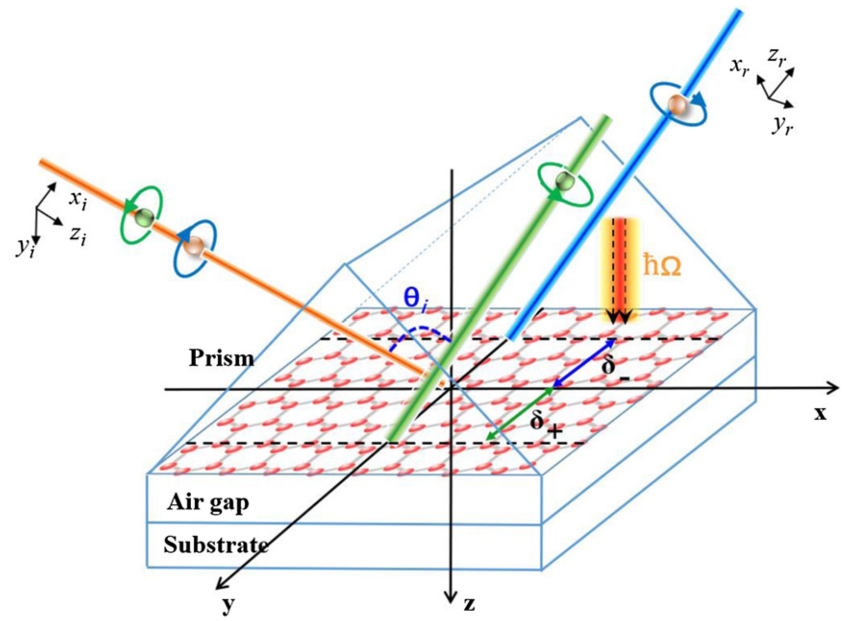

Figure 1. Schematic diagram of the photonic SHE of reflected light in a graphene-dielectric structure. The external optical pumping is applied by low intensity continuous wave laser source with a wavelength of 632.8 nm.

potential application of photonics and optoelectronics due to their extraordinary electronic and photonic properties. Among them, graphene, a single layer of carbon atoms arranged in a hexagonal honeycomb lattice, has the unique electronic and optical properties in infrared and terahertz regions [24, 25]. In particular, its conductivity can be flexibly modulated by external electrostatic field biasing, chemical doping as well as magnetic field. Therefore, graphene has the potential to overcome the aforementioned drawbacks of photonic SHE. Until now, many studies on the modulation and enhancement of photonic SHE have been reported in various nanostructures containing graphene [7, 19, 26–28].

In fact, graphene has been confirmed to host the nonlinear optical properties [29–31], which provides a new platform to explore the effects including nonlinear self-action surface plasmon polariton [32], vector plasmonic lattice soliton [33] and asymmetric plasmonic supermode [34]. In addition, the design of graphene-based lasers and plasmonic amplifiers in terahertz range may be possible owing to the population inversion (a negative conductivity) of graphene under optical pumping [35, 36]. Here, a natural question arises: can we tune the photonic SHE in graphene-based structures by optical pumping?

In this work, we propose a flexible method to achieve a tunable photonic SHE in terahertz region by means of adjustable optical properties of graphene under weak optical pumping. We find that the spin shift of graphene-dielectric structure can be enhanced by applying the external optical pumping on graphene. Moreover, this spin shift is quite sensitive to the pumping power and it can reach its upper limitation (i.e. half of the beam waist) under the optimal pumping power. Such a giant spin shift is associated with the zero value of the real part of graphene conductivity and its large ratio of $|r_{\mathrm{s}}|/|r_{\mathrm{p}}|$. Therefore, our work reveals a convenient way to manipulate the photonic SHE of graphene-based structure by optical pumping, which may provide a new paradigm for tunable spin-based photonic devices.

2. Theory and model

The proposed graphene-dielectric structure is shown in figure 1, in which the refractive indices of both the glass prism and the dielectric substrate is 1.5 and the thickness of air gap is 400 nm. When a linearly polarized beam is incident into the structure with an angle θ_{i}, the reflected beam will split into left- and right-handed circularly polarized spin components, whose centroids shift reversely away from the incident plane. In our configuration, the incident plane is x–z and the transverse shift is along y-axis.

The photonic SHE is usually described by a general propagation model using angular spectrum theory. We consider an incident Gaussian beam whose angular spectrum can be written as:

$$\tilde{\boldsymbol{E}}_{\mathrm{i}} = \frac{w_0}{\sqrt{2\pi}} \exp[-\frac{(k_x^2 + k_y^2)w_0^2}{4}] \tag{1}$$

where w_0 is the beam waist, k_x and k_y are the components of the wave vector along the x and y directions, respectively. The angular spectrum of reflected beam can be expressed as [37]:

$$\begin{bmatrix}\tilde{\boldsymbol{E}}_{\mathrm{r}}^{H}\\ \tilde{\boldsymbol{E}}_{\mathrm{r}}^{V}\end{bmatrix}=\begin{bmatrix} r_{\mathrm{p}} & \dfrac{k_{\mathrm{r}y}\ \cot\ \theta_{\mathrm{i}}(r_{\mathrm{p}}+r_{\mathrm{s}})}{k_0}\\ -\dfrac{k_{\mathrm{r}y}\ \cot\ \theta_{\mathrm{i}}(r_{\mathrm{p}}+r_{\mathrm{s}})}{k_0} & r_{\mathrm{s}}\end{bmatrix}\begin{bmatrix}\tilde{\boldsymbol{E}}_{\mathrm{i}}^{H}\\ \tilde{\boldsymbol{E}}_{\mathrm{i}}^{V}\end{bmatrix} \tag{2}$$

in which $\tilde{\boldsymbol{E}}_{\mathrm{r}}^{H,V}$ and $\tilde{\boldsymbol{E}}_{\mathrm{i}}^{H,V}$ are the H and V components of the angular spectrum for the reflected and incident beams, respectively. r_{p} and r_{s} are Fresnel reflection coefficients for p and s waves. k_0 is the wave number in free space and $k_{\mathrm{r}y}$ is y component of reflected wave vector.

Considering the first-order Taylor series of the Fresnel coefficients, the spin-dependent shifts of the two spin components can be simplified as [13]:

$$\delta_{\pm}^{H}=\mp\frac{k_0w_0^2\ \mathrm{Re}(1+r_{\mathrm{s}}/r_{\mathrm{p}})\cot\ \theta_{\mathrm{i}}}{k_0^2w_0^2+|\frac{\partial\ \ln\ r_{\mathrm{p}}}{\partial\theta_{\mathrm{i}}}|^2+|(1+r_{\mathrm{s}}/r_{\mathrm{p}})\cot\ \theta_{\mathrm{i}}|^2} \tag{3}$$

$$\delta_{\pm}^{V}=\mp\frac{k_0w_0^2\ \mathrm{Re}(1+r_{\mathrm{p}}/r_{\mathrm{s}})\cot\ \theta_{\mathrm{i}}}{k_0^2w_0^2+|\frac{\partial\ \ln\ r_{\mathrm{s}}}{\partial\theta_{\mathrm{i}}}|^2+|(1+r_{\mathrm{p}}/r_{\mathrm{s}})\cot\ \theta_{\mathrm{i}}|^2} \tag{4}$$

where δ^{+} and δ^{-} represent the transverse displacement of left- and right-circularly polarized components, respectively. Since the Fresnel coefficients (r_{p} and r_{s}) are the crucial parameters to determine the value of spin shifts, they can be obtained by [38]:

$$r_A=\frac{r_A^{12}+r_A^{234}\ \mathrm{e}^{2\mathrm{i}k_{2z}d_2}}{1+r_A^{12}r_A^{234}\ \mathrm{e}^{2\mathrm{i}k_{2z}d_2}} \tag{5}$$

where,

$$r_A^{234}=\frac{r_A^{23}+r_A^{34}\ \mathrm{e}^{2\mathrm{i}k_{3z}d_3}}{1+r_A^{23}r_A^{34}\ \mathrm{e}^{2\mathrm{i}k_{3z}d_3}} \tag{6}$$

$$r_p^{m,m+1}=\frac{\varepsilon_{m+1}k_{m,z}-\varepsilon_m k_{m+1,z}}{\varepsilon_{m+1}k_{m,z}+\varepsilon_m k_{m+1,z}} \tag{7}$$

$$r_s^{m,m+1}=\frac{k_{m,z}-k_{m+1,z}}{k_{m,z}+k_{m+1,z}} \tag{8}$$

where $m\in 1,2,3,4$ and $k_{m,z}=k_0\sqrt{\varepsilon_m-\varepsilon_1(\sin\ \theta_{\mathrm{i}})^2}$. 1, 2, 3 and 4 correspond to prism, graphene layer, air gap layer and dielectric substrate, respectively. $A\in$ p, s. $r_{\mathrm{p}}^{m,m+1}$ and $r_{\mathrm{s}}^{m,m+1}$ represent the reflection coefficients of p-polarized and s-polarized light at the interface between m and $m+1$ medium, respectively.

3. Tunable conductivity of graphene via optical pumping

The relative equivalent permittivity of graphene layer can be described by [39]

$$\varepsilon_g=1+\frac{\mathrm{i}\sigma_{\mathrm{g}}\eta_0}{k_0\Delta} \tag{9}$$

where the thickness of monolayer graphene Δ is 0.34 nm, η_0 is the impedance of air, $k_0=2\pi/\lambda$ and λ is the wavelength of the incident wave in the air. The THz conductivity of monolayer graphene consists of two parts: the intraband σ_{intra} and the interband conductivity σ_{inter}, which can be expressed as [40]:

$$\sigma_{\mathrm{intra}}=\frac{2e^2k_{\mathrm{B}}T\tau}{\pi\hbar^2(1+\omega^2\tau^2)}\cdot\log\left(1+\exp\left(\frac{E_{\mathrm{f}}}{k_{\mathrm{B}}T}\right)\right)+\mathrm{i}\frac{2e^2k_{\mathrm{B}}T\omega}{\pi\hbar^2(\omega^2+1/\tau^2)}\cdot\log\left(1+\exp\left(\frac{E_{\mathrm{f}}}{k_{\mathrm{B}}T}\right)\right) \tag{10}$$

$$\sigma_{\mathrm{inter}}=\frac{e^2}{4\hbar}\cdot\tanh\left(\frac{\hbar\omega-2E_{\mathrm{f}}}{4k_{\mathrm{B}}T}\right)+\mathrm{i}\frac{e^2}{8\hbar\pi}\cdot\log\left(\frac{(\hbar\omega+2E_{\mathrm{f}})^2}{(\hbar\omega)^2+(2k_{\mathrm{B}}T)^2}\right) \tag{11}$$

where e represents the charge, k_{B} is the Boltzmann constant, $\hbar$ is the reduced Planck's constant, ω is the angular frequency of incident THz wave, $\tau=3\times10^{-12}$ s is the intraband transition time and E_{f} denotes the electron (hole) Fermi energy at the temperature of T. In case of weak optical pumping ($\eta_{\mathrm{F}}=E_{\mathrm{f}}/(k_{\mathrm{B}}T)<1$), the normalized carrier Fermi energy can be presented as [35]:

$$\eta_{\mathrm{F}}=12\alpha(\frac{\hbar v_{\mathrm{F}}}{k_{\mathrm{B}}T})^2\frac{\tau_{\mathrm{R}}I_{\Omega}}{\hbar\Omega} \tag{12}$$

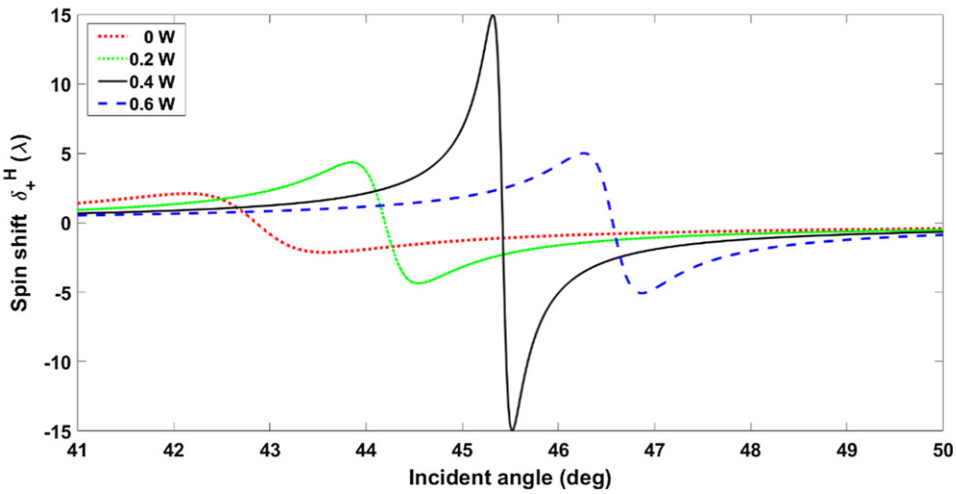

Figure 2. Theoretical calculation of the spin shift versus incident angle under the optical pumping power of 0 W, 0.2 W, 0.4 W and 0.6 W (the beam area is 0.196 mm^2 [29]).

where $\alpha = 1/137$ is the fine structure constant, I_Ω describes the intensity of incident pumping radiation with photon energy of $\hbar\Omega$, $v_F = 10^6$ m s^{-1} is the Fermi velocity of charge carriers in graphene, $\tau_R = 10^{-9}$ s is the characteristic recombination time for electron–hole pairs and T is taken to be 290 K.

It is obvious that η_F (or E_f) can be tuned by the external pumping strength I_Ω, which affects the optical properties of graphene as well as the Fresnel coefficients. In the following, we will study the modulation of photonic SHE in this graphene-dielectric structure by optical pumping with different pumping intensities. Here, low intensity continuous wave laser source with central wavelength of 632.8 nm is chosen as external optical pumping.

4. Photonic spin Hall effect under optical pumping

The influence of optical pumping on the photonic SHE of graphene-dielectric structure is presented in figure 2, which shows the spin shifts versus incident angle for the H polarized incident beam at the frequency of 5 THz with the beam waist of 30λ and it is normalized to the wavelength of incident beam λ. For simplicity, we only show the spin shift for left-handed circularly polarized component since the spin shifts for left- and right-circularly polarized light are opposite in sign and with the same values. It can be seen that with the increase of incident angle, the spin shift increases to a positive maximum value and then decreases to zero at Brewster angle. After that, the spin shift increases to another negative maximum and the absolute value of spin shift decreases. Such variation can be attributed to the change of Fresnel coefficient r_p, which declines to zero and changes sign when the incident angle crosses through the Brewster angle [26]. Moreover, we find that when the external optical pumping is applied on graphene the spin shift can be significantly enhanced in comparison with the case of without optical pumping. The maximal value of spin shift is highly sensitive to the power of optical pumping. Therefore, we suggest a flexible and effective method to manipulate the photonic SHE of graphene-dielectric structure by optical pumping, where the spin shift can be tuned by the power of optical pumping other than the parameters of device structures. Our results remain valid when air gap is replaced by other dielectric materials, whose spin shift keeps the similar profile but with the modified peak position and the optimal pumping power.

To further reveal the effect of optical pumping on photonic SHE of graphene-dielectric structure, the color map of the spin shifts is displayed in figure 3 versus the pumping power and incident angle. From figures 3(a) and (b), we can see that the Brewster angle increases monotonically with the power of optical pumping increasing. For example, the Brewster angle is about 44.5° under the pumping power of 0.3 W and it increases to 46.3° at 0.6 W. Furthermore, the spin shift is so tiny ($<2\lambda$) when the pumping power is less than 0.2 W, then it rapidly increases to about 15λ (its upper limitation, i.e. half of the beam waist) under the power of 0.4 W. After that, the spin shift decreases again and it becomes too small to be observed as the power increases to 0.7 W. Thus, the optimal pumping power is 0.4 W for this graphene-dielectric structure to achieve the giant spin shift of H polarized incident beam, whose maximum value appears at the incident angle of about 45.4°. Figure 3(c) shows the ratio $|r_s|/|r_p|$ as a function of the optical pumping power. It is easy to find that the giant spin shift under optimal power may be attributed to the large ratio of $|r_s|/|r_p|$,

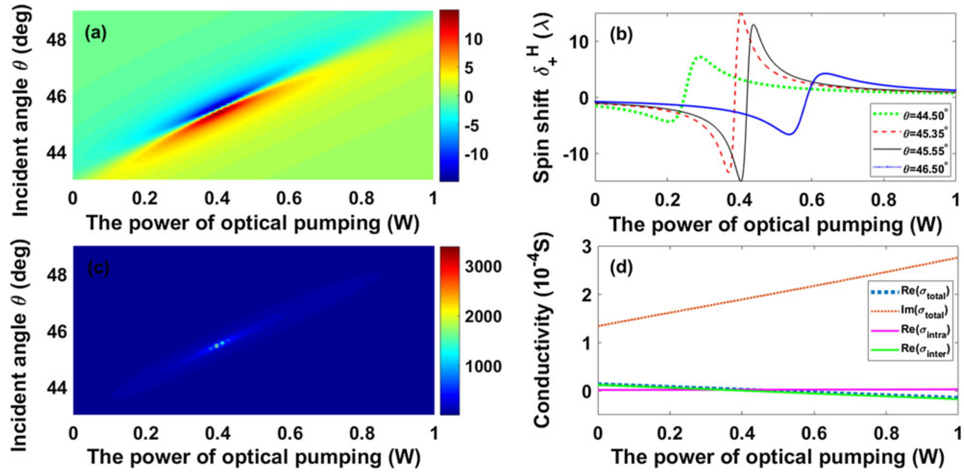

Figure 3. (a) Spin shift and (c) the ratio $|r_s|/|r_p|$ versus the optical pumping power (from 0 to 1 W) and incident angle. (b) The spin shift versus the pumping power under different incident angles. (d) The conductivity of monolayer graphene versus the pumping power.

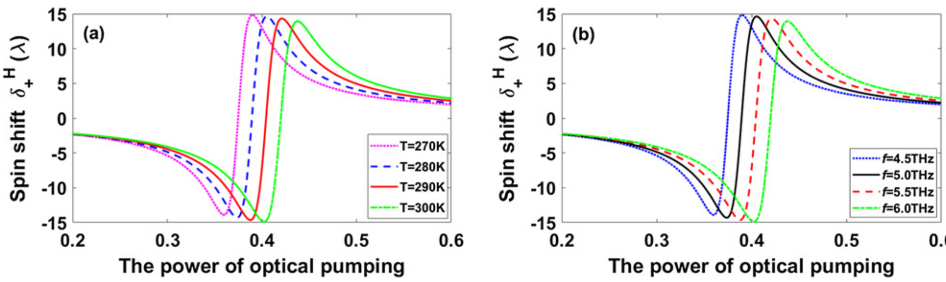

Figure 4. The spin shift versus the optical pumping power with (a) different temperatures and (b) different incident frequencies.

where a large reflection of s-polarized light and a small reflection of p-polarized light happen at the pumping power of 0.4 W.

Figure 3(d) shows the conductivity of graphene as a function of the optimal pumping power. With the power of optical pumping increasing, the imaginary part of total conductivity increases while its real part decreases gradually and changes from positive to negative. For the intraband optical conductivity of graphene, its real part stabilizes to be zero and is independent of the pumping power. Thus, the real part of the total optical conductivity of graphene is mainly determined by the interband contribution. It is noted that the real part of graphene conductivity is equal to zero at the pumping power of 0.4 W, which corresponds to the transition point from positive value to negative one in the spectrum of total optical conductivity of graphene. In addition, $|r_p|$ has the minimum value at this exact transition point, which grants a large ratio of $|r_s|/|r_p|$. One can draw a conclusion that the giant photonic SHE under the optimal pumping power of 0.4 W can be traced back to the zero value of real part of graphene conductivity.

From equations (10) and (11), temperature is a tunable parameter to control the conductivity of graphene. Therefore, the effect of temperature on the spin shift has also been investigated, as illustrated in figure 4(a). By increasing the temperature, the maximum value of the spin shift is almost stable, but the corresponding optimal pumping power increases monotonically. For example, when the temperature equals 270 K the value of spin shift ranges from -13.9λ to 14.9λ with the optimal pumping power of about 0.38 W. In comparison, when we increase the temperature to 300 K, the value of spin shift would change from -14.9λ to 13.9λ and the optimal power is increased to 0.44 W. As a result, temperature might be used as a tuning factor for photonic SHE. In order to achieve a considerable spin shift, the optimal pumping power should be accordingly changed with temperature in the practical application of photonic devices.

The results can also be extended to other incident frequencies. The dependence of spin shift on pumping power at different frequencies is plotted in figure 4(b). It is obvious that the peak position of the spin shift moves toward the right with increasing incident frequencies, indicating the increase of optimal pumping power.

5. Conclusion

In this paper, we theoretically investigate the photonic SHE of graphene-dielectric structure in terahertz region when the weak optical pumping is applied on graphene. It is found that the spin shift can be modulated and enhanced by optical pumping. In particular, the spin shift for H polarized incident beam can achieve its upper limitation (i.e. half of the beam waist) under the optimal pumping power. Such a giant spin shift can be related to the transition point of the real part of graphene conductivity from positive to negative value, which results in a large ratio of $|r_s|/|r_p|$. Therefore, we propose a new paradigm to flexibly control the photonic SHE of graphene-dielectric structure in terahertz range. Our results may open up a new pathway for a tunable spin-based photonic device.

Acknowledgment

This work was supported by National Natural Science Foundation of China (NSFC Grants No. 11774179), Jiangsu Specially Appointed Professor Plan (Grant No. RK033STP16002), Natural Science Foundation of Jiangsu Province (Grant Nos. BK20161513 and BK20171440), Six Categories of Summit Talents of Jiangsu Province of China (Grant No. 2016-JNHB-060), Training program of the Key and Major Research plan of NUPT (NY217166), NUPTSF (NY215027), 1311 Plan, Major Program of Natural Science Foundation by the Ministry of Education of China (TJ215009) and Postgraduate Research & Practice Innovation Program of Jiangsu Province (SJKY19_0779).

ORCID iDs

Jie Cheng https://orcid.org/0000-0001-8415-4071

References

[1] Onada M, Murakami S and Nagaosa N 2004 *Phys. Rev. Lett.* **93** 083901
[2] Sinova J, Culcer D, Niu Q, Sinitsyn N A, Jungwirth T and Macdonald A H 2004 *Phys. Rev. Lett.* **92** 126603
[3] Bliokh K Y, Rodríguez-Fortuño F J, Nori F and Zayats A V 2015 *Nat. Photon.* **9** 796–808
[4] Bliokh K Y and Bliokh Y P 2006 *Phys. Rev. Lett.* **96** 073903
[5] Cardano F and Marrucci L 2015 *Nat. Photon.* **9** 776–8
[6] Aiello A 2012 *New J. Phys.* **14** 013058
[7] Li J, Tang T, Luo L and Yao J Q 2018 *Carbon* **134** 293–300
[8] Kapitanova P V *et al* 2014 *Nat. Commun.* **5** 3226
[9] Aiello A, Lindlein N, Marquardt C and Leuchs G 2009 *Phys. Rev. Lett.* **103** 100401
[10] Hosten O and Kwiat P 2008 *Science* **319** 787–90
[11] Luo H L, Zhou X X, Shu W X, Wen S C and Fan D Y 2011 *Phys. Rev.* A **84** 043806
[12] Qiu X, Zhang Z, Xie L, Qiu J, Gao F and Du J 2015 *Opt. Lett.* **40** 1018–21
[13] Tan X-J and Zhu X-S 2016 *Opt. Lett.* **41** 2478–81
[14] Xiang Y, Jiang X, You Q, Guo J and Dai X 2017 *Photon. Res.* **5** 467–72
[15] Zhou X X, Lin X, Xiao Z C, Low T, Alù A, Zhang B L and Sun H D 2019 *Phys. Rev.* B **100** 115429
[16] Fu Y Y, Fei Y, Dong D X and Liu Y W 2019 *Front. Phys.* **14** 62601
[17] Zhu W and She W 2015 *Opt. Lett.* **40** 2961–4
[18] Lin Y M *et al* 2019 *Opt. Exp.* **27** 15868
[19] Cai L, Liu M X, Chen S Z, Liu Y C, Shu W X, Luo H L and Wen S C 2017 *Phys. Rev.* A **95** 013809
[20] Zhou X X, Zhang J, Ling X H, Chen S Z, Luo H L and Wen S C 2013 *Phys. Rev.* A **88** 053840
[21] Jia G Y, Huang Z X, Ma Q Y and Li G 2020 *Nanophotonics* **9** 715–23
[22] Lin H, Chen B, Yang S, Zhu W, Yu J, Guan H, Lu H, Luo Y and Chen Z 2018 *Nanophotonics* **7** 1929–37
[23] Zhang W, Wu W, Chen S, Zhang J, Ling X, Shu W, Luo H and Wen S 2018 *Photon. Res.* **6** 511–6
[24] Novoselov K S, Geim A K, Morozov S V, Jiang D, Zhang Y, Dubonos S V, Grigorieva I V and Firsov A A 2004 *Science* **306** 666
[25] Castro Neto A H, Guinea F, Peres N M R, Novoselov K S and Geim A K 2009 *Rev. Mod. Phys.* **81** 109–62
[26] Bai X, Tang L, Lu W, Wei X, Liu S, Liu Y, Sun X, Shi H and Lu Y 2017 *Opt. Lett.* **42** 4087–90
[27] Gao C and Guo B 2018 *Optik* **158** 850–4
[28] Cheng M, Fu P, Tang X, Chen S, Chen X, Lin Y and Feng S 2018 *J. Opt. Soc. Am.* B **35** 1829–35
[29] Grebenchukov A N, Azbite S E, Zaitsev A D and Khodzitsky M K 2019 *J. Magn. Magn. Mater.* **472** 25–8
[30] Mikhailov S A 2007 *Europhys. Lett.* **79** 27002
[31] Hendry E, Hale P J, Moger J, Savchenko A K and Mikhailov S A 2010 *Phys. Rev. Lett.* **105** 097401
[32] Gorbach A V 2013 *Phys. Rev.* A **87** 013830
[33] Wang Z, Wang B, Wang K, Long H and Lu P 2016 *Opt. Lett.* **41** 3619–22
[34] Wang F, Wang Z, Qin C, Wang B, Long H, Wang K and Lu P 2017 *Opt. Express* **25** 1234–41
[35] Ryzhii V and Otsuji T M 2007 *J. Appl. Phys.* **101** 083114
[36] Gierz I *et al* 2015 *J. Phys.: Condens. Matter* **27** 164204
[37] Luo H L, Ling X H, Zhou X X, Shu W X, Wen S C and Fan D Y 2011 *Phys. Rev.* A **84** 033801
[38] Jiang X, Wang Q, Guo J, Chen S, Dai X and Xiang Y J 2018 *Plasmonics* **13** 1467–73
[39] Vakil A and Engheta N 2011 *Science* **332** 1291–4
[40] Weis P, Garcia-Pomar J L and Rahm M 2014 *Opt. Express* **22** 8473–89